40 Gb/s PAM-4 Transmitter IC for Long-Wavelength VCSEL Links

Wouter Soenen, Renato Vaernewyck, Xin Yin, *Member, IEEE*, Silvia Spiga, Markus-Christian Amann, *Fellow, IEEE*, Kamalpreet S. Kaur, Paraskevas Bakopoulos, *Member, IEEE* and Johan Bauwelinck, *Member, IEEE*

***Abstract*—Conventional 850 nm multi-mode fiber (MMF) links deployed in warehouse-scale data centers will be limited by modal dispersion beyond 10 Gb/s when covering distances up to 1 km. This can be resolved by opting for a single-mode fiber (SMF), but typically requires the use of power-hungry edge-emitting lasers. We investigate the feasibility of a high-efficiency SMF link by reporting a 0.13 µm SiGe BiCMOS laser diode driver optimized for long-wavelength vertical-cavity surface-emitting lasers (VCSEL). Bit-error rate experiments at 28 Gb/s and 40 Gb/s up to 1 km of SMF reveal that four-level pulse amplitude modulation (PAM-4) can compete with non-return-to-zero (NRZ) in terms of energy efficiency and scalability. With 9.4 pJ/bit, the presented transmitter paves the way for VCSEL-based SMF links in data centers.**

***Index Terms*—BiCMOS integrated circuits, driver circuits, optoelectronic devices, vertical-cavity surface-emitting lasers, amplitude modulation, equalizers.**

I. Introduction

SCALE out networking in data centers has the potential to leverage the proliferating demand for higher aggregate bandwidth. As such, expanding computing and storage power leads to a linear growth in commodity devices instead of upgrading existing hardware [1]. Complete virtualization of the server infrastructure is a necessity to support this cost-effective topology. However, this is accompanied by interconnections that must span the complete data center area where the distance to be covered can rise up to 1 or even 2 km.

Recent research is focusing primarily on directly modulated 850 nm vertical-cavity surface-emitting laser (VCSEL) links for multi-mode fiber (MMF) since this type of link is most commonly deployed in data center networks. A data rate up to 64 Gb/s over 57 m of OM4 MMF is already achieved using non-return-to-zero (NRZ) [2]. Other implementations explore multi-level modulation formats to increase the maximum transmission distance, e.g. error-free operation at 40 Gb/s with four-level pulse amplitude modulation (PAM-4) is obtained after 100 m of OM4 MMF [3]. Characterized by a modal bandwidth of 4.7 GHz and propagation loss of 2.3 dB after bridging 1 km, OM4 MMF will likely be the limiting factor when targeting data rates beyond 10 Gb/s in virtualized data centers.

These drawbacks are significantly less present in a single-mode fiber (SMF) link. Currently, edge-emitting lasers are typically utilized for SMF applications. However, these suffer from a high operating current and are externally modulated to achieve high bit rates [4]. Long-wavelength VCSELs provide a more efficient alternative. Albeit these VCSELs are currently not as fast as their 850 nm counterparts, modulation bandwidths in excess of 15 GHz were published for 1550 nm devices [5]. In this paper, we present a PAM-4 driver IC with on-chip equalization optimized for long-wavelength VCSELs. The transmitter allows us to evaluate the performance of PAM-4 relative to NRZ using the same IC for various lengths of VCSEL-based SMF links.

II. PAM-4 VCSEL transmitter

The presented transmitter IC is capable of driving a 1550 nm common-anode VCSEL array although the experiments are restricted to one channel. Fig. 1 shows a block diagram of the data path. The PAM-4 drive current for the VCSEL is generated on-chip from two NRZ data streams, respectively referenced as most significant bit (MSB) and least significant bit (LSB). A conventional PAM-4 driver topology is used which combines the MSB and LSB currents (i_{msb}, i_{lsb}) at the output node [6]. A unity-gain current buffer at the output prevents capacitive loading from the VCSEL bias current source (i_{bias}) and isolates the MSB and LSB main drivers from each other. The voltage difference between the driver supply (*vdd1*) and VCSEL anode supply (*vdd2*) was exploited to provide extra bias current for the laser. Pulse width distortion (PWD) introduced by the asymmetric response of the VCSEL can be partially corrected by introducing an offset voltage to the predrivers (*PWD control*).

A high-quality PAM-4 signal puts additional timing constraints on the transmitter which makes the design more

Manuscript received xxxxx xx, 20xx; revised xxxxxx xx, 20xx; accepted xxxxx xx, 20xx. Date of publication xxxxxx xx, 20xx; date of current version xxxxxx xx, 20xx.

This work was supported by the European Commission through the FP-7 project Mirage.

W. Soenen, R. Vaernewyck, X. Yin and J. Bauwelinck are with the Department of Information Technology, Ghent University/imec, Sint-Pietersnieuwstraat 41, B-9000 Gent, Belgium (e-mail: wouter.soenen@intec.ugent.be; renato.vaernewyck@intec.ugent.be; xin.yin@intec.ugent.be; johan.bauwelinck@intec.ugent.be).

S. Spiga and M.-C. Amann are with the Walter Schottky Institut, Technische Universität München, Am Coulombwall 4, D-85748 Garching, Germany (email: silvia.spiga@wsi.tum.de; amann@wsi.tum.de).

K. S. Kaur is with the Centre for Microsystems Technology, imec/Ghent University, Technologiepark 914A, B-9052 Gent, Belgium (email: Kaur.Kamalpreet@elis.ugent.be).

P. Bakopoulos is with the Department of Electrical and Computer Engineering, National Technical University of Athens, 9 Iroon Polytechniou Street, 15773 Zografou, Greece (email: pbakop@mail.ntua.gr).

Color versions of one or more of the figures are available online at http://ieeexplore.ieee.org.

Digital Object Identifier xx.xxxx/LPT.201x.xxxxxxx

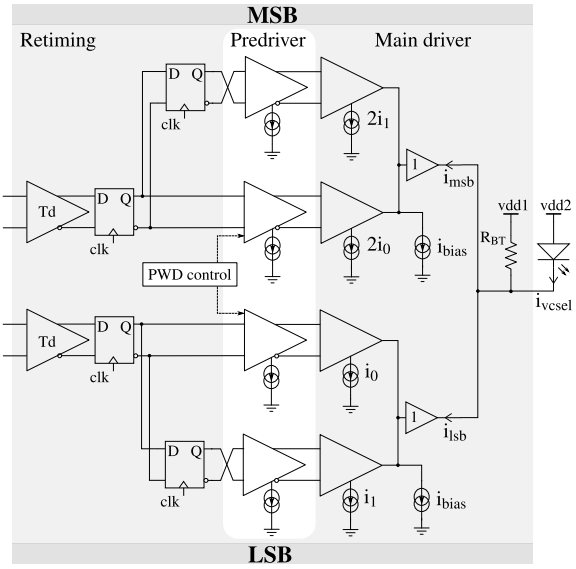

Fig. 1. Simplified block diagram of the data path of the PAM-4 transmitter.

challenging than high-speed NRZ drivers. This requirement is met by retiming the input data with full-rate clock (*clk*) flip flops to ensure that the parallel data streams are synchronized. Programmable delay cells (T_d) are inserted to avoid setup and hold time violation of the retiming block.

1550 nm VCSELs are currently characterized by a modulation bandwidth in excess of 15 GHz [5]. The bandwidth can be extended by pre-emphasizing the VCSEL current (i_{vcsel}) either passively and/or actively. The first method requires on-chip integration of a back termination resistor (R_{BT}) which moves the dominant pole to higher frequencies in exchange for reduced drive efficiency. The other method is based on a feed-forward equalization (FFE) topology consisting of multiple taps to shape the modulation response as desired. This pre-emphasis topology is fully reconfigurable, but takes up additional chip area and sacrifices extinction ratio (ER) for bandwidth enhancement. Knowledge of the bias-dependent optoelectronic (OE) response of the VCSEL is hereby essential in determining the optimal pre-emphasis topology.

Fig. 2a shows that the relaxation resonance is damped as the drive current rises from 6 mA to 10 mA when driven from a 50 Ω source. This type of response can be effectively compensated with a two-tap symbol-spaced FFE architecture similar to [7]. The two tap coefficients correspond to the programmable tail-currents i_0 and i_1 on Fig. 1. Four equally spaced pre-emphasized levels are created by sizing these tail-currents of the MSB and LSB main drivers with a fixed ratio of two. The FFE utilizes the full-rate clock reference from the retiming block and creates the symbol-spaced delay by cascading retiming flip flops. The applied pre-emphasis is therefore independent of the data rate which is not the case for [2] and [8]. The back termination resistor is chosen equal to 50 Ω to obtain the desired damped response necessary for the two-tap FFE such that overshoot is prevent from occurring in the PAM-4 signal. The applied back termination is associated with a drive efficiency of roughly 50 % since the series resistance of the laser varies between 50 and 60 Ω in the

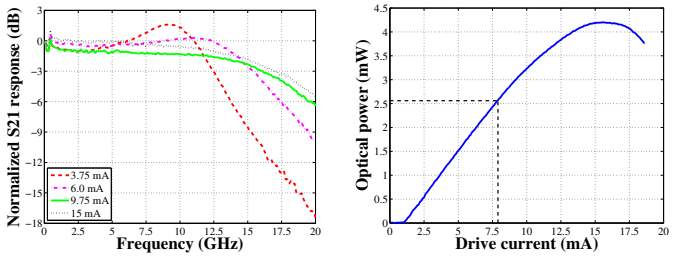

(a) (b)

Fig. 2. Characteristics of a typical 1550 nm VCSEL. (a) S21 modulation response for various bias currents. (b) L/I curve displaying a bias current used in one of the experiments to obtain a damped response.

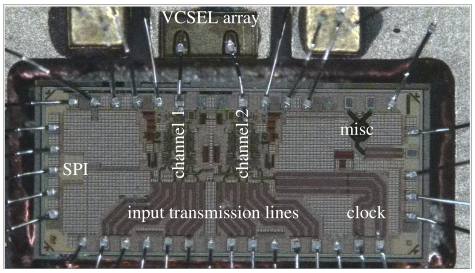

Fig. 3. Micrograph of the transmitter IC and the 1550 nm VCSEL array.

6-10 mA range. Compared to the 50 Ω/120 Ω impedance ratio of the 850 nm VCSEL driver in [2], long-wavelength VCSELs seem to be beneficial in terms of drive efficiency.

III. Experiments

The transmitter IC is fabricated in a 0.13 µm SiGe BiCMOS process. The die measures 2860 µm x 1330 µm and is wire bonded onto a Rogers RO4003C LoPro test board. The length of the bond wires is reduced by mounting the die in a cavity. The driver is able to directly modulate a common-anode VCSEL with PAM-4 or NRZ signals. This functionality allows us to compare the performance of both modulation formats at equal bit rate in a VCSEL-based SMF link for several transmission distances. The type of modulation format generated by the IC depends on the data pattern entering its MSB and LSB inputs. A PAM-4 VCSEL drive current is created by introducing different data patterns in the LSB and MSB inputs, whereas NRZ is generated when the two input data streams are the same. This was implemented experimentally by introducing a delay difference of around half a pseudorandom bit sequence (PRBS) period between the LSB and MSB data streams for PAM-4 or synchronizing both data streams with each other for NRZ. The AC-coupled MSB and LSB inputs are excited single-endedly with a 2^7-1 PRBS of 300 mV peak-to-peak by an SHF 12100B pattern generator. The transmitter drive current settings are reconfigurable through a serial interface (SPI).

The VCSEL emits light at a wavelength of 1550 nm and was developed by the Technische Universität München. The structure is based on the short-cavity buried tunnel junction (BTJ) concept [5]. The characteristics of the mounted VCSEL with a BTJ diameter of 5 µm are a 3 dB bandwidth exceeding

15 GHz, a series resistance between 50 and 60 Ω , a maximum output power of 4.2 mW and a slope efficiency of 0.35 W/A. The threshold and roll-over current are respectively 1.1 mA and 15 mA. The VCSEL is biased with an average current that can vary between 7.7 and 8.8 mA depending on the experiment. Fig. 3 shows a micrograph of the transmitter IC and the long-wavelength VCSEL array. Nominal supply voltages are 2.5 V for the transmitter (*vdd1*) and 3.85 V for the VCSEL anode (*vdd2*). The light from the VCSEL is captured with a manually aligned flat-cut SMF. Best case alignment trials for the bias condition shown on the L/I curve in Fig. 2b produced an optical power of −2.3 dBm for 4.1 dBm of emitted power. The 6.4 dB coupling loss is primarily caused by the inability of the positioner to control the tilt of the fiber. An erbium-doped fiber amplifier proceeded with an optical attenuator is therefore integrated into the measurement setup to provide the receiver with a constant output power regardless of the alignment problems. The spacing between the consecutive levels of the PAM-4 signal is preserved by operating the 40 G OE receiver from Sumitomo in its linear region. This restricts the average received power to −4 dBm.

The first experiment examines how chromatic dispersion affects the quality of the PAM-4 and NRZ link at 28 Gb/s when covering a distance of 100 m and 1 km. Electrical eye diagrams captured from the receiver with 50 GHz remote sampling heads represent this effect visually while bathtub curves of the horizontal and vertical eye margin attained with the SHF 11100B bit-error rate (BER) analyzer verify this quantitatively. The results acquired in a back-to-back (BTB) configuration after optimization of the applied FFE serve as a reference for this test. The doubling in spectral efficiency of PAM-4 relative to NRZ modulation lets us expect that the latter will experience more deterioration as the distance increases. The differing bandwidth requirements are pronounced by programming the transmitter at maximum drive current for both modulation formats while separately optimizing the pre-emphasis. Remark that the available lab equipment forces us to carry out BER tests solely on the middle eye of the PAM-4 signal which maps to the transmitted MSB data. The settings of the transmitter were optimized such that the upper or lower eye of the measured PAM-4 signal show a comparable eye-opening in our experiments, allowing the measured BER based on the middle eye a fair representation. The second and last experiment explores the maximum bit rate achievable with the PAM-4 VCSEL transmitter and compares the energy efficiency with state-of-the-art 850 nm VCSEL transmitters and an externally modulated laser.

IV. Results and Discussion

At a data rate of 28 Gb/s, the long-wavelength VCSEL starts to introduce ISI due to its limited bandwidth. As can be observed in the eye diagrams of Fig. 4, the on-chip symbol-spaced FFE is able to restore the eye again. However, the applied FFE reduces the optical modulation amplitude (OMA) significantly more for NRZ. This means that the 4.7 dB power penalty associated to PAM-4 is not valid anymore for bandwidth limited links and has dropped to 3.7 dB in this case.

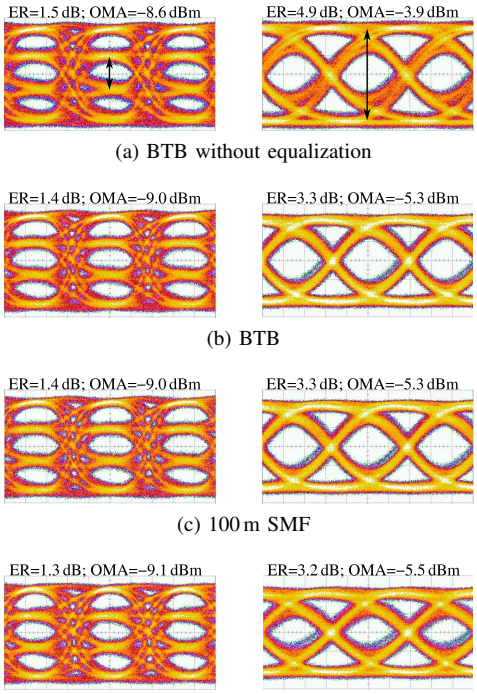

Fig. 4. 28 Gb/s PAM-4 and NRZ received eye diagrams. Vertical scale is 50 mV/div and horizontal scale is 20 ps/div for PAM-4 and 10 ps/div for NRZ diagrams.

The −4 dBm constraint on the received power leads to an OMA of the PAM-4 middle eye which approximates the sensitivity level of the Sumitomo receiver. All qualitative comparisons will therefore be made at a reference BER of 10^{-9} to minimize the impact of the OE receiver sensitivity. The bathtub curves in Fig. 5 show that FFE restores NRZ eye height and width with respectively 30 % and 17 % and makes the PAM-4 link back error free. The inherent asymmetric rise and fall times of the VCSEL are not compensated by the FFE as can be derived from the asymmetric shape of the bathtub curves and eye diagrams. Expanding the transmission distance to 100 m and 1 km reveals that both modulation formats experience a similar reduction in time margin which amounts 35 % at 1 km compared to the BTB case. There is however a significant penalty offset noticeable in vertical eye margin. At 100 m, the NRZ eye height is compressed with 10 % which even drops to 60 % for 1 km of SMF. A decline of less than 5 % in eye height confirms our expectations that PAM-4 is much more rigid against chromatic dispersion than NRZ in directly modulated VCSEL links. Although the BER results show that NRZ still beats PAM-4 in terms of absolute performance, it has to be noted that only a decisive conclusion can be drawn when the receiver is separately optimized for each modulation scheme. Parameters such as sensitivity, pre-emphasis and dispersion will further reduce the power penalty related to PAM-4 as the bit rate continues to rise. The stringent timing margin of NRZ will also play a role in choosing the most efficient topology for the future data center link.

Error-free performance was maintained up to 40 Gb/s in a BTB PAM-4 setup as shown in Fig. 6. The BER rises to 10^{-11} and 10^{-9} as the transmission distance progresses from 100 m

TABLE I
COMPARISON OF THE STATE OF THE ART IN OPTOELECTRONIC TRANSMITTERS

Reference	[9]	[8]	[2]	[4]	**This work**
Technology	32 nm SOI CMOS	0.13 µm SiGe	0.13 µm SiGe	150 GHz InP-DHBT	0.13 µm SiGe
Bit rate (Gb/s)	35	40	64	56	40
Modulation format	NRZ	NRZ	NRZ	NRZ	PAM-4
Laser bandwidth (GHz)	N/A	16	26	35	>15
Supply voltage (V)	1.1/3.1	2.5/3.3	N/A	-5.2	2.5/3.85
Energy efficiency (pJ/bit)	1.3	7.8	14.1	26.8	9.4
Wavelength (nm)	850 nm	850 nm	850 nm	1300 nm	1550 nm

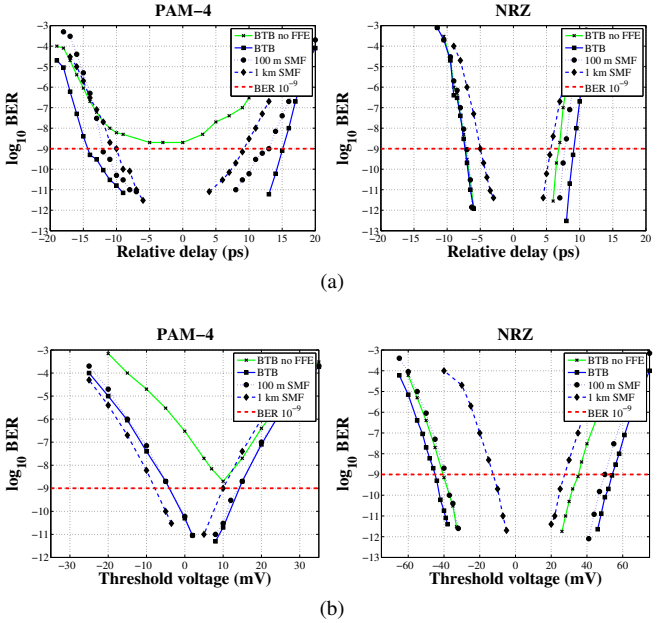

Fig. 5. Measured bathtub curves at 28 Gb/s PAM-4 and NRZ modulation for several lengths of SMF. (a) Horizontal eye margin. (b) Vertical eye margin.

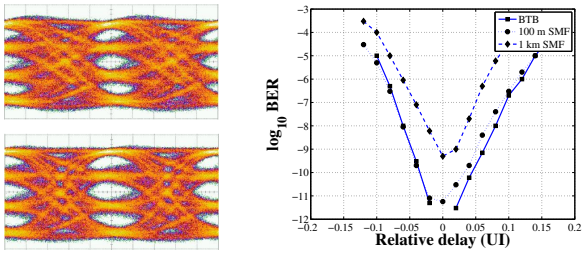

Fig. 6. 40 Gb/s PAM-4 transmission experiment. (a) Received eye diagram in BTB setup (bottom) and after 1 km of SMF (top), 50 mV/div, 10 ps/div. (b) Bathtub curve of horizontal eye margin for several configurations.

to 1 km. Described by an energy efficiency of 9.4 pJ/bit, the presented PAM-4 VCSEL transmitter is able to compete with the state-of-the-art SiGe BiCMOS 850 nm NRZ transmitters [2], [8] listed in Table I. It is almost three times more efficient than a long-wavelength transmitter consisting of an electro-absorption modulated edge-emitting laser [4]. The CMOS driver reports the best efficiency of them all [9], but the four-stage design (no FFE) is far less complex compared to our design and 32 nm SOI CMOS is a much more advanced process than 0.13 µm SiGe BiCMOS.

V. CONCLUSION

We have demonstrated a SiGe BiCMOS PAM-4 transmitter targeting high-efficiency 1550 nm VCSEL-based SMF links. Its potential for warehouse-scale data center applications is confirmed by evaluating multiple transmission distances at 28 Gb/s. The NRZ link showed a severe compression in eye height after 1 km of fiber while the PAM-4 link was negligibly affected. The bit rate of the long-wavelength VCSEL link could be extended to 40 Gb/s by using on-chip symbol-spaced FFE. Characterized by an energy efficiency of 9.4 pJ/bit, the presented PAM-4 VCSEL driver proves to be a scalable and efficient alternative to traditional NRZ transmitters consisting of 850 nm VCSELs or edge-emitting lasers.

ACKNOWLEDGMENT

The authors would like to thank D. Frederickx and L. Viaene from imec for wire bonding the transmitter board and Sumitomo Electric Device Innovations for the OE 40 G receiver module.

REFERENCES

[1] A. Vahdat, "Delivering scale out data center networking with optics – Why and how," in *Opt. Fiber Commun. Conf.*, Los Angeles, CA, USA, 2012, pp. 1–36.
[2] D. Kuchta, A. V. Rylyakov, C. L. Schow, J. Proesel, C. Baks, P. Westbergh, J. S. Gustavsson, and A. Larsson, "64Gb/s Transmission over 57m MMF using an NRZ Modulated 850nm VCSEL," in *Opt. Fiber Commun. Conf.*, San Francisco, CA, USA, 2014, p. Th3C.2.
[3] P. Westbergh, M. Karlsson, A. Larsson, P. Andrekson, and K. Szczerba, "60 Gbits error-free 4-PAM operation with 850 nm VCSEL," *Electron. Lett.*, vol. 49, no. 15, pp. 953–955, Jul. 2013.
[4] T. Tatsumi, K. Tanaka, S. Sawada, H. Fujita, and T. Abe, "1.3 μm, 56-Gbit/s EML Module target to 400GbE," in *Opt. Fiber Commun. Conf.*, Washington, D.C., USA, 2012, p. OTh3F.4.
[5] M. Muller, W. Hofmann, T. Grundl, M. Horn, P. Wolf, R. D. Nagel, E. Ronneberg, G. Bohm, D. Bimberg, and M. C. Amann, "1550-nm High-Speed Short-Cavity VCSELs," *IEEE J. Sel. Topics. Quantum Electron.*, vol. 17, no. 5, pp. 1158–1166, Sep. 2011.
[6] D. Watanabe, A. Ono, and T. Okayasu, "CMOS optical 4-PAM VCSEL driver with modal-dispersion equalizer for 10Gb/s 500m MMF transmission," in *IEEE Int. Solid-State Circuits Conf. - Dig. Tech. Pap.*, Los Angeles, CA, Feb. 2009, pp. 106–107,107a.
[7] M. Bruensteiner, G. Papen, J. Poulton, S. Tell, R. Palmer, K. Giboney, D. Dolfi, and S. Corzine, "3.3-V CMOS pre-equalization VCSEL transmitter for gigabit multimode fiber links," *IEEE Photon. Technol. Lett.*, vol. 11, no. 10, pp. 1301–1303, Oct. 1999.
[8] Y. Tsunoda, M. Sugawara, H. Oku, S. Ide, and K. Tanaka, "8.9 A 40Gb/s VCSEL over-driving IC with group-delay-tunable pre-emphasis for optical interconnection," in *IEEE Int. Solid-State Circuits Conf. Dig. Tech. Pap.*, San Francisco, CA, USA, Feb. 2014, pp. 154–155.
[9] J. Proesel, B. G. Lee, C. W. Baks, and C. Schow, "35-Gb/s VCSEL-Based Optical Link using 32-nm SOI CMOS Circuits," in *Opt. Fiber Commun. Conf.*, Anaheim, CA, USA, 2013, p. OM2H.2.